

# Scalable Nonlinear Spectral Dimensionality Reduction (NLSDR) Methods For Streaming Data

Suchismit Mahapatra



# Manifold Learning In Streams

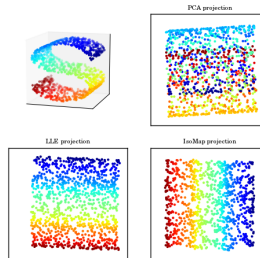
## Motivation

- Understanding the **structure** of multidimensional **patterns** is of **primary** importance.
- Processing data streams, potentially **infinite** requires adequate **summarization** which can **handle inherent constraints** and **approximate characteristics** well.

# Manifold Learning In Streams

Massive amounts of data

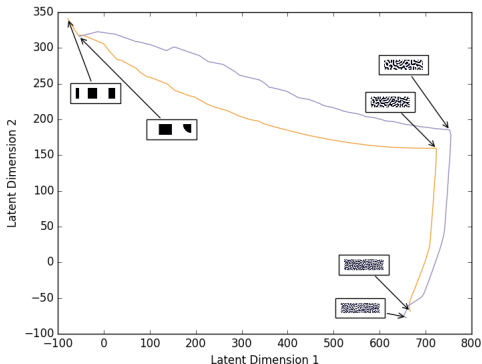
- Natural data tends to be generated by systems (physical or non-physical) that have **very few** degrees of underlying freedom.
- Real-world data is typically a result of **complex non-linear processes**, but can often be described by a **low-dimensional manifold**.



[Credit: Raymond Fu]

# Manifold Learning In Streams

## Nonlinear Process Dynamics



Morphological parametric trajectories for a nonlinear process.

[Click here for simulation of all parametric trajectories] [Click here for simulation of Manifold]

# Manifold Learning In Streams

## Challenges Involved

- Curse of dimensionality combined with lack of scalability of algorithms makes data analysis difficult/inadequate.
- Cannot use entire streams as training data motivates Out-of-Sample Extension (OOSER) techniques.
- Need to formalize “collective error” in NLSDR methods and strategies to quantify it.
- Dealing with intersecting manifolds.
- Need to handle concept drift i.e. changes in stream properties.

# Learning efficiently

## Common Approaches

- Smoothness
  - Try to learn functions that are **smooth**.
  - Examples - Spline based techniques, Kernel methods,  $L_2$ -regularization, etc.
- Sparsity
  - Represent in terms of **sparse/few** basis functions.
  - Examples - Lasso, Compressive Sensing, Wavelets
- Geometry
  - Data distribution is **not uniform**, try to **exploit geometry**.
  - Examples - Laplacian based techniques, Manifold learning

Even more **relevant** in high-dimensional spaces.

# Manifold Learning

## Assumptions

- Distribution of data **not uniform**.
- Data **lives on/near** some low-dimensional manifold, typically embedded in high dimensions and **separated** by **low-density regions**.
- Typically used as a generic **non-linear, non-parametric technique** to **approximate** probability distributions in high-dimensional spaces.

# Manifold

## Properties

### Definition

A manifold  $\mathcal{M}$  is a metric space with the following property: if  $x \in \mathcal{M}$ , then there exists some neighborhood  $\mathcal{U}$  of  $x$  and  $\exists n$  such that  $\mathcal{U}$  is homeomorphic to  $\mathbb{R}^n$ .

# Manifold

## Properties

### Definition

A manifold  $\mathcal{M}$  is a metric space with the following property: if  $x \in \mathcal{M}$ , then there exists some neighborhood  $\mathcal{U}$  of  $x$  and  $\exists n$  such that  $\mathcal{U}$  is homeomorphic to  $\mathbb{R}^n$ .

- Global structure can be more complicated.
- Usually embedded in high dimensional spaces, but the intrinsic dimensionality is typically low due to fewer degrees of freedom.
- Examples
  - Set of queries/product descriptions
  - Image data sets
  - State space of MDP's

# Manifold

## Caltech 101 Dataset



[Credit: <https://lvdmaaten.github.io/>]

# Nonlinear Spectral Dimension Reduction

## Formulation

### Definition

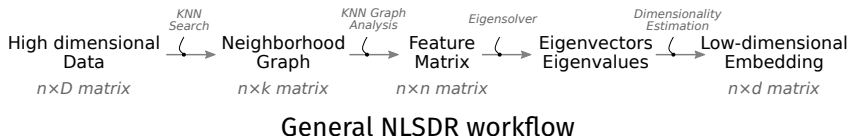
Given  $X = [\mathbf{x}_1, \mathbf{x}_2, \dots, \mathbf{x}_n]^\top$ , where  $\forall \mathbf{x}_i \in \mathbb{R}^D$ , the task is to **find** a corresponding **low-dimensional** representation,  $\mathbf{y}_i \in \mathbb{R}^d$ , for each  $\mathbf{x}_i$ , where  $d \ll D$ .

- We assume there **exists**  $\phi : \mathbb{R}^d \rightarrow \mathbb{R}^D$  that **maps** each data sample  $\mathbf{y}_i \in \mathbb{R}^d$  to  $\mathbf{x}_i \in \mathbb{R}^D$ .
- The goal is to **learn the inverse mapping**,  $\phi^{-1}$ , that can be used to map high-dimensional  $\mathbf{x}_i$  to low-dimensional  $\mathbf{y}_i$ , i.e.  $\mathbf{y}_i = \phi^{-1}(\mathbf{x}_i)$ .

# Nonlinear Spectral Dimension Reduction

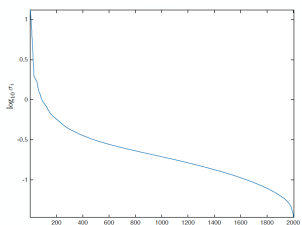
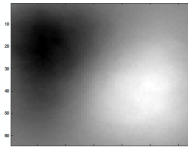
## Overview & Workflow

- NLSDR techniques i.e. Isomap, Diffusion Maps, Laplacian Eigenmaps, Locally Linear Embedding rely on the **spectral decomposition** of the feature matrix that captures properties of the **underlying sub-manifold**.



# Nonlinear Spectral Dimension Reduction

## Illustration



PCA on a simple data set and the intrinsic dimensionality it uncovers, even after using Fourier transformation.

[Credit: Mauro Maggioni]

# Nonlinear Spectral Dimension Reduction

## Isomap

- Isomap is a **non-linear** generalization of the classical **Multi Dimensional Scaling (MDS)** algorithm.
- The intuition is to perform MDS, not in the input space, but rather in the **geodesic space** of the non-linear data manifold.
- But there are **plenty of challenges** to manifold learning.

# S-Isomap

## Notion of Error

- To measure the notion of error, we use Procrustes analysis.
- The idea is to align matrices,  $\mathcal{A}$  and  $\mathcal{B}$ , by finding the optimal translation  $t$ , rotation  $\mathcal{R}$ , and scaling  $s$  that minimizes the Frobenius norm between  $\mathcal{A}$  and  $\mathcal{B}$ :

$$\epsilon_{proc}(\mathcal{A}, \mathcal{B}) = \min_{\mathcal{R}, t, s} \|s\mathcal{R}\mathcal{B} + t - \mathcal{A}\|_F.$$

# S-Isomap

## Notion of Error

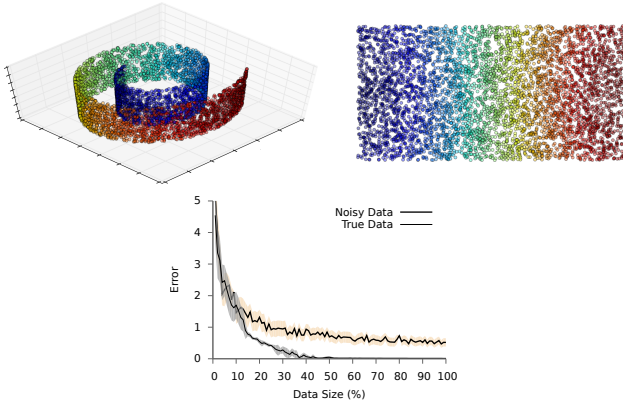
- To measure the notion of error, we use **Procrustes analysis**.
- The idea is to align matrices,  $\mathcal{A}$  and  $\mathcal{B}$ , by finding the **optimal** translation  $t$ , rotation  $\mathcal{R}$ , and scaling  $s$  that minimizes the Frobenius norm between  $\mathcal{A}$  and  $\mathcal{B}$ :

$$\epsilon_{proc}(\mathcal{A}, \mathcal{B}) = \min_{\mathcal{R}, t, s} \|s\mathcal{R}\mathcal{B} + t - \mathcal{A}\|_F.$$

- The above has a **closed form solution** obtained by performing SVD on  $\mathcal{A}\mathcal{B}^T$ .
- We determine how well  $LDE_{\mathcal{X}}$  represents the low-dimensional ground truth  $GT_{\mathcal{X}}$  using  $\epsilon_{proc}(LDE_{\mathcal{X}}, GT_{\mathcal{X}})$ .

# S-Isomap

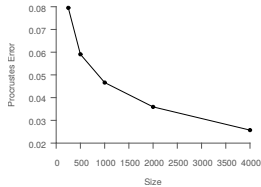
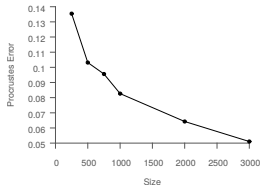
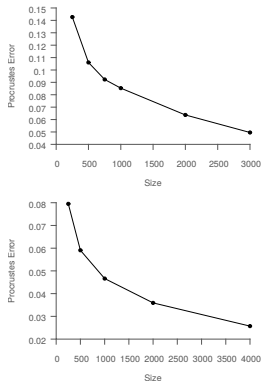
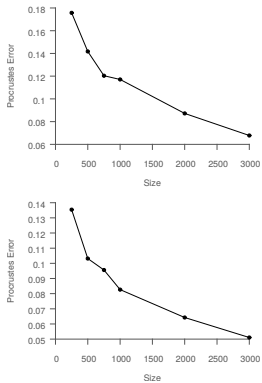
## Notion of Error



Procrustes error between the true and approximate mapping learnt with and without sampling error.

# S-Isomap

Experiments using MNIST, Corel, Swiss Roll datasets



We actually need a much smaller dataset to adequately form a robust manifold structure !!

# S-Isomap

## Algorithm Design

This key intuition allowed us to formulate a **much cheaper** means for mapping streaming points to the manifold.

- ① Choose an **initial batch set**  $\mathcal{B}$  based on error analysis.
- ② Perform exact Isomap (or other NLSDR) on  $\mathcal{B}$  to get the manifold  $\mathcal{M} = LDE_{\mathcal{B}}$ .
- ③ Subsequently, **map** streaming points  $s \in \mathcal{S}$  by **matching their inner products** with  $LDE_{\mathcal{B}}$  to the computed geodesic distances with the  $k$  nearest neighbors of  $s$ .

# S-Isomap

## Proposed Algorithm

---

Input:  $G_b, X_b, Y_b, \mathbf{x}_s, k$

Output:  $\mathbf{y}_s$

---

- 1: **kNN, kDist**  $\leftarrow \text{KNN}(\mathbf{x}_s, X_b, k)$
- 2: **for**  $1 \leq i \leq n$  **do**
- 3:    $\mathbf{g}_i \leftarrow \min_{1 \leq j \leq k} \{\mathbf{kDist}_j + G_{b_{\text{kNN}_j, i}}\}$
- 4: **end for**
- 5:
- 6:  $\mathbf{c} \leftarrow \frac{1}{2}(\bar{\mathbf{g}} \cdot \mathbf{1}_n - \mathbf{g} - \bar{\mathbf{G}}_b \cdot \mathbf{1}_n + \bar{\mathbf{G}}_b)$
- 7:  $\mathbf{p} \leftarrow (Y_b^\top Y_b)^{-1} Y_b^\top \mathbf{c}$
- 8:  $\hat{Y} \leftarrow [Y_b; \mathbf{p}]$
- 9:  $\mathbf{y}_s \leftarrow \mathbf{p} - \hat{Y}$
- 10: **return**  $\mathbf{y}_s$

---

# S-Isomap

## Performance analysis

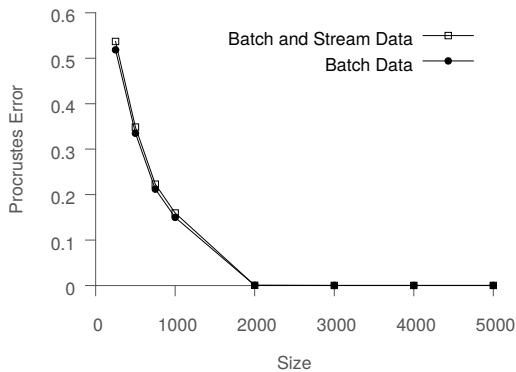
Method	Time Complexity
OOSE (non-incremental)	$\mathcal{O}(m * (n^2 \log(n) + n^2 k))$
OOSE (incremental)	$\mathcal{O}(\sum_{i=1}^{m+n} (iD + i^2 \log(i) + i^2 k))$
S-Isomap	$\mathcal{O}(n^3 + mn(D + d^2 + k))$

$$n = |B|, m = |S|, n \ll m$$

OOSE above refers to the out-of-sample-extension technique proposed by Law and Jain (2006). S-Isomap has a  $\mathcal{O}(\max(n^2, nd))$  space complexity.

# S-Isomap

## Results for Euler Isometric Swiss Roll



The results illustrate that the error due to streaming points is low as well as similar asymptotic behavior.

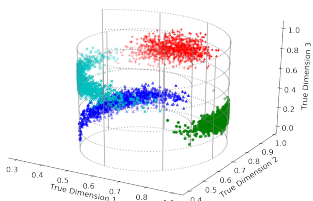
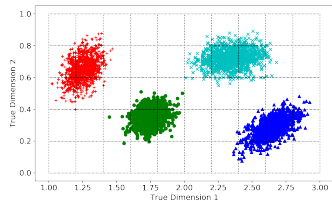
# S-Isomap

## Summary

- We studied & formulated the **notion of error metrics** for manifold learning techniques and quantified them, as well as we **devise** a technique to deal with scenarios wherein **ground truth** is **unavailable**.
- We demonstrate that it is **possible to learn** a robust, stable manifold using only a **subset of data**.
- Consequently, we propose a novel **incremental, online** algorithm, suitable for **high-volume, high-throughput stream processing**, to incorporate streamed data into a **stable** manifold, efficiently.

# S-Isomap++

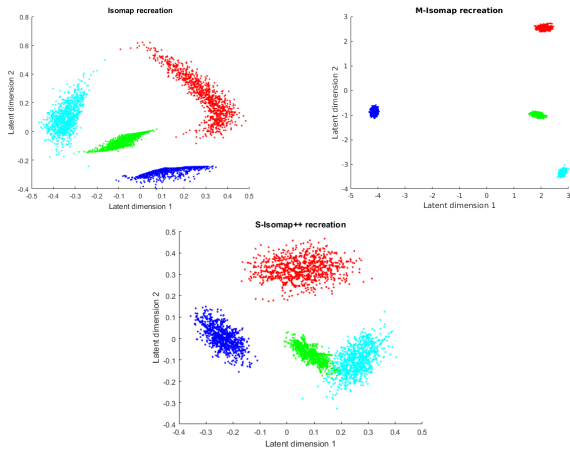
## Motivation



Typical real world scenario wherein we need to learn the inverse mapping,  $\phi^{-1}$ , to be able to uncover the intrinsic low-dimensional representation from high-dimensional data.

# S-Isomap++

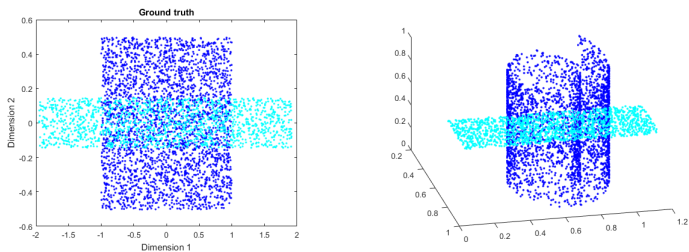
## Motivation



How well different algorithms could recreate the latent ground truth used to generate the high-dimensional data.

# S-Isomap++

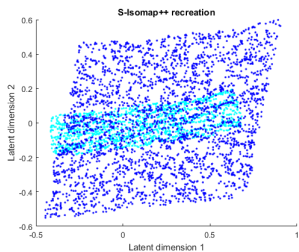
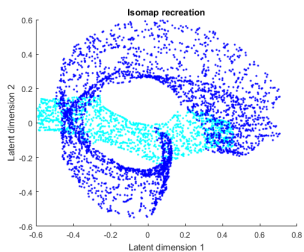
## Motivation



Multiple manifolds typically involve **dissimilar mappings**  $\{\phi_i\}_{i=1,2,\dots,p}$  projecting the intrinsic low-dimensional representation to higher dimensional real-world data.

# S-Isomap++

## Motivation



In an ideal scenario, when manifolds are **densely sampled** and **sufficiently separated**, existing NLSDR methods can uncover individual manifolds. But **intersecting** manifolds are still a challenge.

# S-Isomap++

## Introduction

The algorithm takes in as input, the batch and streaming data sets,  $\mathcal{B}$  and  $\mathcal{S}$  respectively and can be divided into two main phases:

- Batch processing phase
  - Cluster samples in  $\mathcal{B}$  into  $p$  clusters.
  - Learn individual manifolds corresponding to each cluster, and map samples from each cluster to its low-dimensional representation.
  - Map low-dimensional samples from individual manifolds into a global space.
- Stream mapping phase
  - Map each sample  $s$  from  $\mathcal{S}$  onto each of the  $p$  manifolds by matching their inner products to the computed geodesic distances with the  $k$  nearest neighbors, to determine which manifold  $s$  belongs to.

# S-Isomap++

## Batch Processing phase

---

```

1:  $\mathcal{C}_{i=1,2,\dots,p} \leftarrow \text{Find\_Clusters}(\mathcal{B}, \epsilon)$ 
2:  $\xi_s \leftarrow \emptyset$ 
3: for  $1 \leq i \leq p$  do
4:    $\mathcal{LDE}_i \leftarrow \text{Isomap}(\mathcal{C}_i)$ 
5: end for
6:  $\xi_s \leftarrow \bigcup_{i=1}^p \bigcup_{j=i+1}^p \text{NN}(\mathcal{C}_i, \mathcal{C}_j, k) \cup \text{FN}(\mathcal{C}_i, \mathcal{C}_j, l)$ 
7:  $\mathcal{GE}_s \leftarrow \text{MDS}(\xi_s)$ 
8: for  $1 \leq j \leq p$  do
9:    $\mathcal{I} \leftarrow \xi_s \cap \mathcal{C}_j$ 
10:   $\mathcal{A} \leftarrow \begin{bmatrix} \mathcal{LDE}_j^{\mathcal{I}} \\ e^T \end{bmatrix}$ 
11:   $\mathcal{R}_i, t_i \leftarrow \mathcal{GE}_{\mathcal{I}, s} \times \mathcal{A}^T (\mathcal{A} \mathcal{A}^T + \lambda I)^{-1}$ 
12: end for

```

# S-Isomap++

## Tangent Manifold Clustering

- Multiscale SVD (M-SVD) allows us to estimate the intrinsic dimension of noisy, high-dimensional point clouds.
- M-SVD estimates the intrinsic dimension by computing singular values  $\sigma_{i \in \{1, 2, \dots, D\}}^{x, r}$  of  $\mathcal{B}(x, r)$ ,  $\forall x \in \mathcal{M}$ , at different scales  $r > 0$ .

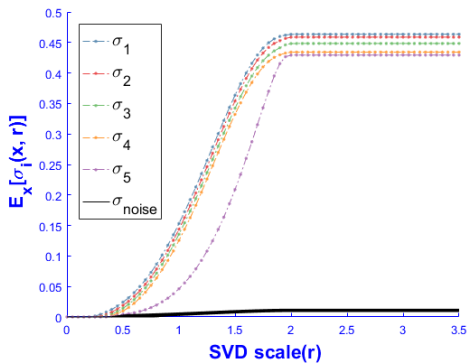
# S-Isomap++

## Tangent Manifold Clustering

- Multiscale SVD (M-SVD) allows us to estimate the intrinsic dimension of noisy, high-dimensional point clouds.
- M-SVD estimates the intrinsic dimension by computing singular values  $\sigma_{i \in \{1, 2, \dots, D\}}^{x, r}$  of  $\mathcal{B}(x, r)$ ,  $\forall x \in \mathcal{M}$ , at different scales  $r > 0$ .
- Small  $r$  leads to not enough samples in  $\mathcal{B}(x, r)$ .
- Large  $r$  leads to curvature making the process over estimate the intrinsic dimension.
- True  $\{\sigma_i^{x, r}\}$  separate from the noise  $\{\sigma_i^{x, r}\}$  at the right scale, due to their different rates of growth and the intrinsic dimension of  $\mathcal{M}$  gets revealed.

# S-Isomap++

## Tangent Manifold Clustering



How  $\{\sigma_i^{x,r}\}$  behave over different scales when M-SVD is done on a noisy  $\mathbb{R}^5$  sphere embedded in  $\mathbb{R}^{100}$  ambient space. Notice how the noise dimensions decay out, leaving only the primary components at the appropriate scale.

# S-Isomap++

## Tangent Manifold Clustering

- Executing M-SVD on the local neighborhood of  $\forall \mathbf{x}_i \in \mathcal{B}$ , allows us to determine basis vectors,  $\mathbf{t}_{i1}, \mathbf{t}_{i2}, \dots, \mathbf{t}_{id'}$ , which define the tangent plane,  $\mathcal{T}_i$ .
- To determine the similarity between tangent planes  $\mathcal{T}_i$  and  $\mathcal{T}_j$ , we tried the following techniques, including two novel approaches :
  - **Gunawan's approach :**  
 $\phi(\mathcal{T}_i, \mathcal{T}_j) = \cos \theta = |\det(\mathcal{N})|$ , where  $\mathcal{N}_{x,y} = \mathcal{T}_{ix}^T \mathcal{T}_{jy}$
  - **$L_1$ -norm based metric :**  
 $\phi(\mathcal{T}_i, \mathcal{T}_j) = \frac{1}{k} \sum_{l=1}^k |\mathbf{t}_{il}^\top \mathbf{t}_{jl}|$
  - **$L_2$ -norm based metric :**  
 $\phi(\mathcal{T}_i, \mathcal{T}_j) = \sqrt{\frac{1}{k} \sum_{l=1}^k (\mathbf{t}_{il}^\top \mathbf{t}_{jl})^2}$

# S-Isomap++

## Tangent Manifold Clustering

- Incremental in nature.
- Initially all points  $\forall \mathbf{x}_i \in \mathcal{B}$  are unlabeled.
- An unlabeled random point  $\mathbf{x}_k$  is picked and is labeled as  $l_k$ , the next available label index.
- Subsequently, similarity of  $\mathbf{x}_k$  with all unlabeled  $x \in \mathcal{N}(\mathbf{x}_k)$  is evaluated. If similarity exceeds certain threshold i.e.  $\cos \theta \geq \epsilon_{thres}$ , points in  $\mathcal{N}(\mathbf{x}_k)$  also get labeled as  $l_k$ .
- Repeat above, till all points are labeled.

# S-Isomap++

## Stream Mapping phase

---

S-Isomap maps points  $s \in \mathcal{S}$  by matching their inner products with  $LDE_{\mathcal{C}_i}$  to the computed geodesic distances with the  $k$  nearest neighbors of  $s$ .

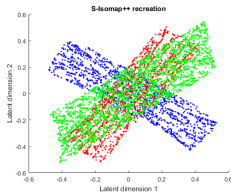
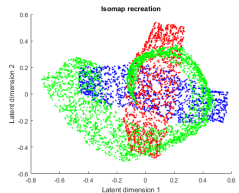
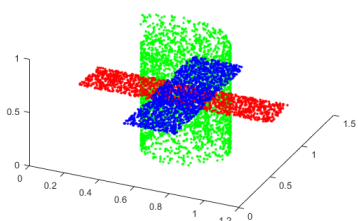
---

```
1: for  $s \in \mathcal{S}$  do
2:   for  $1 \leq i \leq p$  do
3:      $y_s^i \leftarrow S\text{-Isomap}(s, \mathcal{C}_i)$ 
4:      $\mathcal{GE}_s^i \leftarrow \mathcal{R}_i y_s^i + t_i$ 
5:   end for
6: end for
7: index  $\leftarrow argmin_i |y_s^i - \mu(\mathcal{C}_i, \mathcal{R}_i, t_i)|$ 
8:  $\mathcal{Y}_{\mathcal{S}} \leftarrow \mathcal{Y}_{\mathcal{S}} \cup y_s^{index}$ 
9: return  $\mathcal{Y}_{\mathcal{S}}$ 
```

---

# S-Isomap++

## Multiple planes through swiss-roll



Top: Actual manifolds in  $\mathbb{R}^3$  space, clustered for demonstration, Bottom Left: ↗

# S-Isomap++

## Results

<i>Method</i>	<i>L-1</i>	<i>L-2</i>	<i>Gunawan</i>
Sphere-Sphere	<b>0.825</b>	0.619	0.5
Sphere-Plane	<b>0.759</b>	0.602	0.5
Swiss Roll-Plane	<b>0.838</b>	0.621	0.5

Accuracy scores for the different tangent manifold clustering approaches.

digit '0'	<b>0.0296</b>	digit '3'	<b>0.0364</b>	digit '6'	<b>0.0476</b>
digit '1'	<b>0.0806</b>	digit '4'	<b>0.0586</b>	digit '8'	<b>0.0712</b>
digit '2'	<b>0.0499</b>	digit '5'	<b>0.0449</b>	digit '9'	<b>0.0498</b>

Procrustes error values for different digits of MNIST, computed by comparing the original with 3-D recreation via S-Isomap++.

# S-Isomap++

## Summary

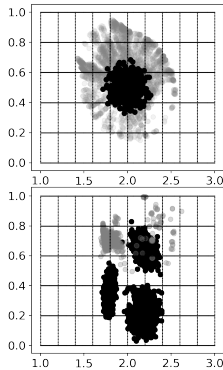
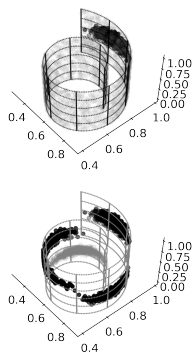
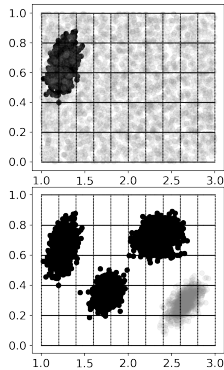
- The proposed algorithm allows for **scalable** non-linear dimensionality reduction of **streaming high-dimensional data**.
- By allowing for the samples to belong to **multiple** manifolds, or sampled **non-uniformly** in a single manifold, our approach can be applied to a **wide variety of practical** settings.
- The ability to **cluster** data lying on **multiple intersecting** manifolds is **significant** since it allows us to **automatically** identify the number of **underlying** manifolds.
- Our algorithm **assumes** that all manifolds are represented in the batch data set. This means that a novel manifold which might **appear** subsequently in the stream  $\mathcal{S}$ , does not get learned. We plan to **resolve** this limitation in our **future work**.

# GP-Isomap

## Motivation

Handling non-stationary streams:

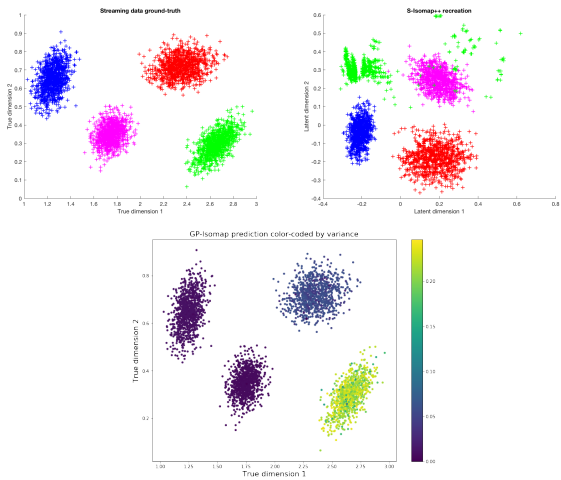
- S-Isomap++ cannot detect and handle changes in the stream distribution.



# GP-Isomap

## Motivation

- **Fits** a GP on batch data.
- **Computes** GP predictions on streaming samples.
- **Uses GP variance** to identify possible shifts in stream.
- Subsequently, **re-trains** batch to handle novel instances.



# GP-Isomap

## Methodology

- Uses Isomap for learning low-dimensional embeddings for  $\mathbf{C}_{i=1,2\dots p}$ .
- For hyper-parameter estimation, uses low-dimensional embeddings uncovered by Isomap and Geodesic Distance based kernel.
- For Gaussian Process (GP) regression, uses low-dimensional embeddings uncovered by Isomap, Geodesic Distance based kernel and GP specific estimated hyper-parameters.

# GP-Isomap

## Batch Phase

### Batch phase of GP-Isomap

```

1:  $\mathcal{C}_{i=1,2,\dots,p} \leftarrow \text{Find-Clusters}(\mathcal{B}, \epsilon)$  FN( $\mathcal{C}_i, \mathcal{C}_j, l$ )
2:  $\xi_s \leftarrow \emptyset$ 
3: for  $1 \leq i \leq p$  do
4:    $\mathcal{LDE}_i, \mathcal{G}_i \leftarrow \text{Isomap}(\mathcal{C}_i)$ 
5: end for
6: for  $1 \leq i \leq p$  do
7:    $\phi_i^{GP} \leftarrow \text{Estimate}(\mathcal{LDE}_i, \mathcal{G}_i)$ 
8: end for
9:  $\xi_s \leftarrow \bigcup_{i=1}^p \bigcup_{j=i+1}^p \text{NN}(\mathcal{C}_i, \mathcal{C}_j, k) \cup$ 
10:  $\mathcal{GE}_s \leftarrow \text{MDS}(\xi_s)$ 
11: for  $1 \leq i \leq p$  do
12:    $\mathcal{I} \leftarrow \xi_s \cap \mathcal{C}_i$ 
13:    $\mathcal{A} \leftarrow \begin{bmatrix} \mathcal{LDE}_j^{\mathcal{I}} \\ e^T \end{bmatrix}$ 
14:    $\mathcal{R}_i, t_i \leftarrow \mathcal{GE}_{\mathcal{I}, s} \times \mathcal{A}^T (\mathcal{A}\mathcal{A}^T + \lambda I)^{-1}$ 
15: end for

```

# GP-Isomap

## Streaming Phase

### Streaming phase of GP-Isomap

```

1:  $\mathcal{S}_u \leftarrow \emptyset$                                 9:   if  $\sigma_j \leq \sigma_t$  then
2: for  $s \in \mathcal{S}$  do                               10:     $y_s \leftarrow \mathcal{R}_j\mu_j + t_j$ 
3:   if  $|\mathcal{S}_u| \geq n_s$  then                     11:     $\mathcal{Y}_s \leftarrow \mathcal{Y}_s \cup y_s$ 
4:      $\mathcal{Y}_u \leftarrow$  Re-run Batch Phase           12:   else
      with  $\mathcal{B} \leftarrow \mathcal{B} \cup \mathcal{S}_u$           13:      $\mathcal{S}_u \leftarrow \mathcal{S}_u \cup s$ 
5:   end if                                         14:   end if
6:   for  $1 \leq i \leq p$  do                      15:   end for
7:      $\mu_i, \sigma_i \leftarrow$  GP-Reg( $s, \mathcal{LDE}_i, \mathcal{G}_i$ ) 16:   end for
8:      $j \leftarrow \operatorname{argmin}_i |\sigma_i|$           17:   return  $\mathcal{Y}_s$ 

```

# GP-Isomap

## Geodesic-Distance Based Kernel

The GP-Isomap algorithm uses a novel geodesic distance based kernel function defined as:

$$k(\mathbf{y}_i, \mathbf{y}_j) = \sigma_s^2 \exp\left(-\frac{\mathbf{b}_{i,j}}{2\ell^2}\right)$$

where  $\mathbf{b}_{i,j}$  is the  $ij^{th}$  entry of the normalized geodesic distance matrix  $\mathbf{B}$ ,  $\sigma_s^2$  is the signal variance (whose value is fixed as 1.0 in this work) and  $\ell$  is the length scale hyper-parameter.

# GP-Isomap

## Geodesic-Distance Based Kernel

The novel kernel is **positive-definite** (PD) as demonstrated below :-

$$\mathbf{K}(\mathbf{x}, \mathbf{y}) = \mathbf{I} + \sum_{i=1}^d \left[ \exp\left(-\frac{\lambda_i}{2\ell^2}\right) - 1 \right] \mathbf{q}_i \mathbf{q}_i^T = \mathbf{I} + \mathbf{Q} \tilde{\Lambda} \mathbf{Q}^T$$

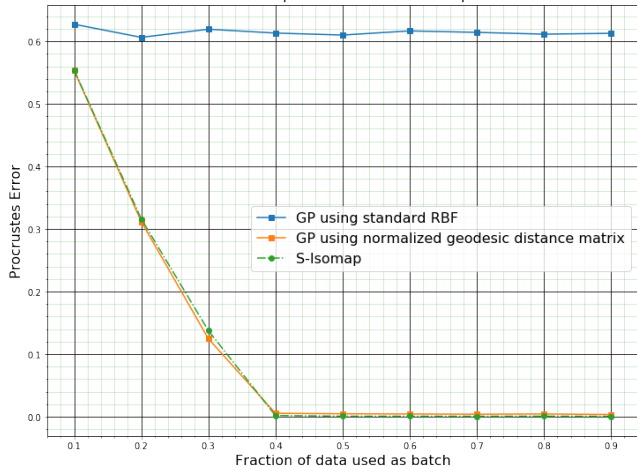
where  $\tilde{\Lambda} = \begin{bmatrix} \left[ \exp\left(-\frac{\lambda_1}{2\ell^2}\right) - 1 \right] & 0 & 0 \\ 0 & \ddots & 0 \\ 0 & 0 & \left[ \exp\left(-\frac{\lambda_d}{2\ell^2}\right) - 1 \right] \end{bmatrix}$  and

$\{\lambda_i, \mathbf{q}_i\}_{i=1\dots d}$  are the **eigenvalue/eigenvector** pairs of  $\mathbf{B}$ .

# GP-Isomap

## Results

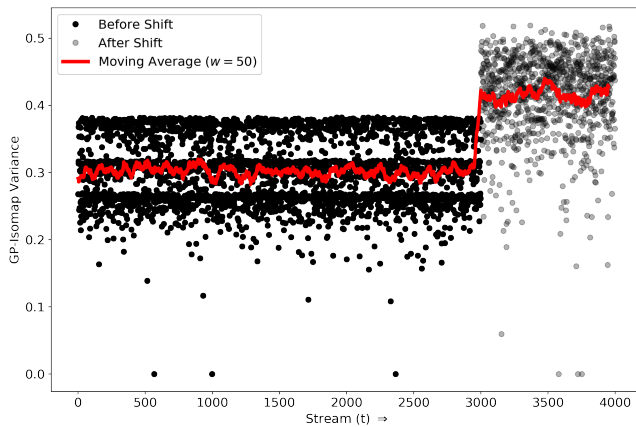
GP-Isomap ~ vanilla GP ~ S-Isomap



[Procrustes error (PE) between the ground truth with a) GP-Isomap (blue line) with the geodesic distance based kernel, b) S-Isomap (dashed blue line with dots) and c) GP-Isomap (green line) using the Euclidean distance based kernel, for different fractions ( $f$ ) of data used in the batch  $\mathcal{B}$ .]

# GP-Isomap

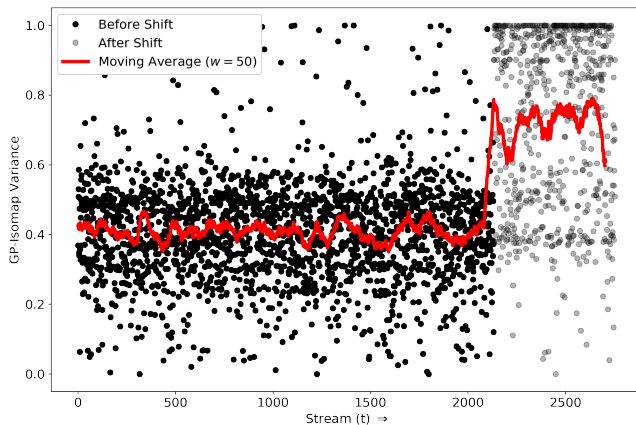
## Results



[Using variance to detect *concept-drift* using the four patches dataset. Initially, when stream consists of samples generated from known modes, variance is low, later when samples from an unrecognized mode appear, variance shoots up. We can also observe the three variance “bands” above corresponding to the variance levels of the three modes for  $t \leq 3000$ .]

# GP-Isomap

## Results



[Using variance to identify concept-drift for the GSAD dataset. The introduction of points from an unknown mode in the stream results in variance increasing drastically as demonstrated by the mean (red line). The spread of variances for points from known modes ( $t \lesssim 2000$ ) is also smaller, compared to the spread for the points from the unknown mode ( $t \gtrsim 2000$ ).]

# S-Isomap

## Theoretical Results

### Theorem

Given uniformly sampled, unimodal distribution from which the batch dataset  $\mathcal{B}$  for S-Isomap is derived from,  $\exists n_0$  i.e. for  $n \geq n_0$  the Procrustes Error  $\epsilon_{\text{Proc}}(\tau_{\mathcal{B}}, \tau_{\text{ISO}})$  between  $\tau_{\mathcal{B}} = \phi^{-1}(\mathcal{B})$ , the true underlying representation and  $\tau_{\text{ISO}} = \hat{\phi}^{-1}(\mathcal{B})$ , the embedding uncovered by Isomap is small ( $\epsilon_{\text{Proc}} \approx 0$ ) i.e. **the batch phase of the S-Isomap algorithm converges**.

### Proof.

- [Bernstein et al.] showed that a data set  $\mathcal{B}$  having samples drawn from a Poisson distribution with density function  $\alpha$  satisfying certain conditions, leads to

$$(1 - \lambda_1) \leq \frac{d_G(x, y)}{d_M(x, y)} \leq (1 + \lambda_2) \quad [\forall x, y \in \mathcal{B}] \quad (1)$$

# S-Isomap

## Theoretical Results

Proof.

- $\tilde{D}_G = \tilde{D}_M + \Delta\tilde{D}_M$
- Equating the expected sample size ( $n\tilde{\alpha}$ ) from a fixed distribution to the density function  $\alpha$ , we get the threshold for  $n_0$  i.e.

$$\begin{aligned} n_0 &= (1/\tilde{\alpha}) \log(V/(\mu\tilde{V}(\delta/4)))/\tilde{V}(\delta/2) \\ &= (1/\tilde{\alpha}) [\log(V/\mu\eta_d(\lambda_2\epsilon/16)^d)]/\eta_d(\lambda_2\epsilon/8)^d \end{aligned} \tag{2}$$

where  $\tilde{D}_M$  and  $\tilde{D}_G$  represent the squared distance matrix corresponding to  $d_M(x, y)$  and  $d_G(x, y)$  respectively,  $\tilde{\alpha}$  is the probability of selecting a sample from  $\mathcal{B}$ ,  $V$  = volume of the manifold,  $\tilde{V}(r) = \eta_d r^d$  and  $\eta_d$  = volume of unit ball in  $\mathbb{R}^d$ .

# S-Isomap

## Theoretical Results

Proof.

- [Sibson et al] demonstrated the robustness of MDS to small perturbations i.e. let  $F$  perturb the true squared-distance matrix  $B$  to  $B + \Delta B = B + \epsilon F$ . PE between the embeddings uncovered by MDS for  $B$  and  $B + \Delta B$  equates to  $\frac{\epsilon^2}{4} \sum_{j,k} \frac{e_j^T F e_k^2}{\lambda_j + \lambda_k} \approx 0$  for small perturbation matrix  $F$ .
- Substituting  $\epsilon = 1$  and replacing  $B$  with  $\tilde{D}_M$  and  $\Delta B$  with  $\Delta \tilde{D}_M$  above, we get our result, since the entries of  $\Delta \tilde{D}_M$  are very small i.e.  $\{0 \leq \Delta \tilde{D}_M(i,j) \leq \lambda^2\}_{1 \leq i,j \leq n}$  where  $\lambda = \max(\lambda_1, \lambda_2)$  for small  $\lambda_1, \lambda_2$ .

# GP-Isomap

## Theoretical Results

### Theorem

*The prediction  $\tau_{GP}$  of GP-Isomap is equivalent to the prediction  $\tau_{ISO}$  of S-Isomap upto translation, rotation and scaling factors i.e. the Procrustes Error  $\epsilon_{Proc}(\tau_{GP}, \tau_{ISO})$  between  $\tau_{GP}$  and  $\tau_{ISO}$  is 0.*

### Proof.

- Want to show  $\epsilon_{Proc}(\tau_{GP}, \tau_{ISO}) = 0$ .
- Subsequently, demonstrate that  $\tau_{GP}$  is a scaled, translated, rotated version of  $\tau_{ISO}$ .

# GP-Isomap

## Theoretical Results

### Proof.

- The 1<sup>st</sup> dimension for S-Isomap prediction can be written as

$$\tau_{\text{ISO1}} = \frac{\sqrt{\lambda_1}}{2} \sum_{i=1}^n \mathbf{q}_{1,i} (\gamma - \mathbf{g}_{i,n+1}^2) \quad (3)$$

- The 1<sup>st</sup> dimension for GP-Isomap prediction can be written as

$$\tau_{\text{GP1}} = \frac{\alpha \sqrt{\lambda_1}}{1 + \alpha \mathbf{c}_1} \sum_{i=1}^n \mathbf{q}_{1,i} \left( 1 - \frac{\mathbf{g}_{i,n+1}^2}{2\ell^2} \right) \quad (4)$$

where  $\gamma = \left( \frac{1}{n} \sum_j \mathbf{g}_{i,j}^2 \right)$ ,  $\lambda_1 = 1^{\text{st}}$  eigenvalue of  $\mathbf{B}$  and  $\mathbf{q}_1$  the corresponding eigenvector,  $\alpha = \frac{1}{(1+\sigma_n^2)}$  and  $\mathbf{c}_1 = [\exp(-\frac{\lambda_1}{2\ell^2}) - 1]$ .

# GP-Isomap

## Theoretical Results

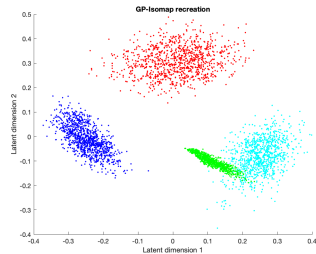
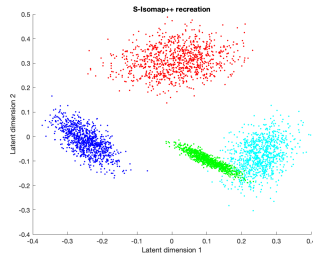
### Proof.

- (3) is a scaled, translated, rotated version of (4).
- Similarly, for each of the dimensions ( $1 \leq i \leq d$ ),  $\tau_{GPi}$  can be shown to be a scaled, translated, rotated version of  $\tau_{ISOi}$ .
- We consolidate these individual scaling, translation and rotation factors together into single collective factors and demonstrate the required result.



# GP-Isomap

## Empirical Results



Comparing predictions for S-Isomap++ and GP-Isomap empirically for the Euler Isometric Swiss Roll data set. The low-dimensional representations uncovered by each are almost similar.

# GP-Isomap

## Summary

- We studied and developed a **systematic approach** which can perform **scalable** and **robust** non-linear dimension reduction of **high-dimensional streaming data**.
- We formulated a **novel geodesic distance based kernel** function and provide an **analysis** of its **spectral** properties.
- Our proposed approach **allows** us to not only **predict** but also **provides** a measure of prediction uncertainty.
- We provide **theoretic results** which allow us to **understand** how **well** our proposed algorithm **works**.

# Current Work

## Conclusions & Future Work

- Can work with only a fraction of the data and still be able to learn, while processing the remaining data "cheaply".
- Demonstrate theoretically that a "point of transition" exists for certain algorithms.
- Provide error metrics to practically identify them.
- Formulate a generalized OOSE framework for streaming NLSDR.
- Including other NLSDR methods as part of this framework and understanding relationships with other members of the NLDR family are future research directions.

# References

## Publications

- Schoeneman, F.\*, Mahapatra, S.\*, Chandola, V., Napp, N., & Zola, J. (2017, June). **Error metrics for learning reliable manifolds from streaming data.** In Proceedings of the 2017 SIAM International Conference on Data Mining (pp. 750-758). Society for Industrial and Applied Mathematics.
- Mahapatra, S., & Chandola, V. (2017, December). **S-Isomap++: Multi manifold learning from streaming data.** In 2017 IEEE International Conference on Big Data (Big Data) (pp. 716-725). IEEE.
- Mahapatra, S., & Chandola, V. (2018). **Learning manifolds from non-stationary streaming data.** arXiv preprint arXiv:1804.08833.

[\* Equal Contribution]